Acta Mechanica 184, 15–31 (2006)
DOI 10.1007/s00707-005-0304-5

Acta Mechanica
Printed in Austria

Vortex shedding suppression for laminar flow past a square cylinder near a plane wall: a two-dimensional analysis

S. Bhattacharyya, Kharagpur, and **D. K. Maiti**, Pilani, India

Received September 12, 2005
Published online: February 6, 2006

Summary. A numerical study on the uniform shear flow past a long cylinder of square cross-section placed parallel to a plane wall has been made. The cylinder is considered to be within the boundary layer of the wall. The maximum gap between the plane wall to the cylinder is taken to be 0.25 times the cylinder height. We investigated the flow when the regular vortex shedding from the cylinder is suppressed. The governing unsteady Navier-Stokes equations are discretized through the finite volume method on staggered grid system. A pressure correction based iterative algorithm, SIMPLER, has been used to compute the discretised equations iteratively. We found that the critical value of the gap height for which vortex shedding is suppressed depends on the Reynolds number, which is based on the height of the cylinder and the incident stream at the surface of the cylinder. At high Reynolds number ($Re \geq 500$) however, a single row of negative vortices occurs for wall to cylinder gap height $L \geq 0.2$. The shear layer that emerges from the bottom face of the cylinder reattaches to the cylinder itself at this gap hight.

1 Introduction

There have been several studies on the behavior of vortex shedding behind an obstacle placed parallel to the ground because of its relevance in practical cases. Typical examples are the vibration of pipelines lying on the sea-bottom under the effect of sea-currents; pipelines and bridges under the effect of the wind, flow past heat exchanger tubes near walls, multiple conductor transmission lines, structures in the atmospheric boundary layers or other significant cases. Vortex shedding causes a noticeable erosion of the support of these structures. The presence of the wall can modify the transport phenomena in the wake. For example, reducing the cylinder-wall separation can lead to a significant augmentation of heat transfer along the wall (Bailey et al. [1]). The presence of the ground modifies the dynamics, with respect to the unbounded conditions, due to essentially three different factors: namely, the impermeability of the wall gives an irrotational constraint to the bluff body wake, the velocity profile in front of the body is notuniform, production of secondary vortex along the ground and the unsteady boundary-layer separation from the wall. When there is a gap between the wall and the body, the onset of vortex formation appears at a critical gap height (Bearman and Zdravkovich [2], Taniguchi et al. [3], Bosch and Rodi [4], Zovatto and Pedrizzetti [5], Price et al. [6], Bailey et al. [1]). The Karman vortex street is formed by concentration of vorticity due to the rolling-up of separated shear layers that issued from both sides of the cylinder. Based on the flow

visualization several authors observed that at small gap ratios the concentration of vorticity is reduced and the formation of vorticity is interrupted by the gap flow mechanisms (Bearman and Zdravkovich [2], Grass et al. [7] and Bosch et al. [9]). Some of the vorticity in the separated shear layer is cancelled by the opposing vorticity in the boundary layer along the wall. The vortex street behind the body consists of an upper row of strong negative vortices and a lower row of weak positive vortices. The physical mechanism and the critical gap height for which vortex shedding is suppressed has been investigated by several authors. Bearman and Zdravkovich [2] predicted that the vortex shedding for a cylinder of circular cross-section near a turbulent boundary layer along a plane wall is suppressed at gap height less than about 0.3 times the cylinder diameter. Grass et al. [7] observed experimentally that at small gap heights the strong recirculation zone which is formed along the wall downstream of the cylinder deflects the flow jet from the gap side away from the wall to form a free jet. This action prevents vortex roll-up in the lower side of the cylinder. Taneda [8] studied the flow around a circular cylinder towed through water past a plane wall. For small gaps between the wall and the cylinder, Taneda [8] observed a single row of negative vortices shed downstream. Price et al. [6] also observed the formation of a single row of negative vortices at gap height 0.25 times the cylinder diameter. There they found the upstream separation bubble for small values of wall to cylinder gap height and for the limiting case, when the cylinder is sited on the wall. Recently, Zovatto and Pedrizzetti [5] made a study on the flow about a circular cylinder placed between two parallel walls. The experimental and numerical studies on the turbulent flow around a square cylinder in the proximity of a wall have been investigated by Bosch et al. [9]. They observed that the influence of the wall resulted in a thinning of the shear layer along the wall side face of the cylinder and a thickening of the shear layer along the upper side of the cylinder. Subsequently Bosch et al. [9] observed through experimental studies that irregular or intermittent vortex shedding occurs for gap heights just larger than the gap height where complete suppression of vortex shedding occurs. Bailey et al. [1] observed that the strength of the upper shear layer increased for wall to cylinder gap height 0.5 times the cylinder height, while the lower shear layer decreased in strength. They concluded that suppression of periodic shedding occurs because of the increasingly different strengths of the shear layers for decreasing gap heights so that the lower shear layer is eventually too weak to couple with the upper one. Recently, Martinuzzi et al. [10] made an experimental study on the influence of wall proximity on vortex shedding from a square cylinder. Through the surface pressure measurement they observed some important differences between the flow around a circular cylinder and the square cylinder for lower values of wall to cylinder gap heights. Liou et al. [11] presented a three-dimensional large eddy simulation of the turbulent wake behind a square cylinder. Their result shows that the celerity of the positive vortex shed from the lower side of the cylinder is smaller than that of the upper side shed vortex due to the interaction with the wall boundary layer.

We find from the above discussions that most of the existing studies on the influence of wall proximity on vortex shedding behind a square cylinder are based on the experimental measurements where the Reynolds number is in the turbulent range, and in this range of Reynolds number the flow is found to be relatively insensitive to the variation of the same. Therefore the dependence of the critical gap height for which vortex shedding is suppressed on the Reynolds number has not been investigated in most of the previous studies discussed before. Another motivation for the present work is that the mechanism of vortex shedding suppression in the laminar or turbulent range of the Reynolds number is made for a circular cylinder (Bearman and Zdravkovich [2], Taneda [8], Lei et al. [12], Zovatto and Peritzzetti [5], Price et al. [6]). For a square cylinder the location of the flow separation is fixed at the upstream corners unlike a circular cylinder, where separation points move back and forth.

The objective of the present paper is to investigate the physical mechanisms for the cessation of vortex shedding and the formation of a steady wake for smaller values of wall to cylinder gap height. The flow is considered to be two-dimensional and laminar. This is bound to miss out many significant features of practical flows, especially three-dimensionality and turbulence, but these features are complex individually let alone acting together. Recently, Bailey et al. [1] examined the three-dimensional nature of turbulent vortex shedding from a square cylinder in the vicinity of a plane wall. There they concluded that for gap heights close to that for vortex shedding suppression the vortex formation process is increasingly two-dimensional. However, it is assumed that the three-dimensional effect would not severely contaminate the results obtained from changing the gap height at a fixed Reynolds number. It has been observed by several authors, as discussed before, that regular vortex shedding is suppressed when a cylinder is placed close to a rigid boundary beyond a gap between the wall and the cylinder of 0.3 times the cylinder height. In order to investigate the wake structure when regular vortex shedding is suppressed, we restricted our investigation for the flow at wall to cylinder gap heights below 0.3 at various values of the Reynolds number. Our result shows that the suppression of vortex shedding depends on the wall to cylinder gap heights as well as on the Reynolds number. An upstream separation bubble appears for small values of wall to cylinder gap height.

2 Governing equations and numerical methods

We consider a plane wall lying along the x-axis, and a long cylinder of square cross-section of height A is placed parallel to the plane wall at a height H from the plane wall (see Fig. 1). We considered that the upstream flow field is due to a uniform shear which is in accord with the boundary-layer theory. We take the prescribed slope λ of the incident velocity profile at the surface multiplied by A, i.e., $U = \lambda A$ as the velocity scale and the height of the cylinder A as characteristic length. Time-dependent, two-dimensional Navier-Stokes equations for a constant property fluid in nondimensional conservative form are given by

$$\frac{\partial u}{\partial x} + \frac{\partial v}{\partial y} = 0, \tag{1}$$

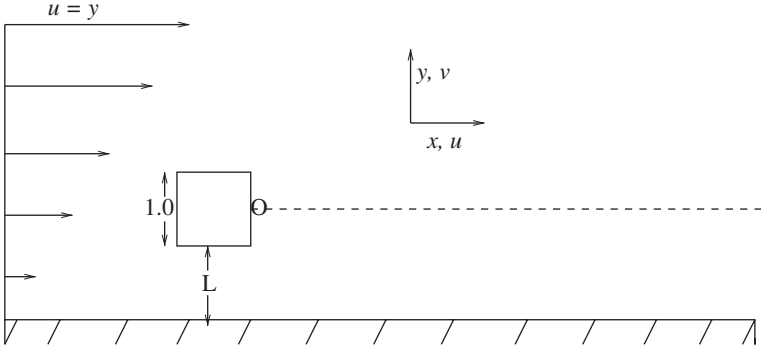

Fig. 1. Schematics of the flow configuration. "o" indicates the location of the monitor point at which the time history of the velocity field is evaluated

$$\frac{\partial u}{\partial t}+\frac{\partial u^2}{\partial x}+\frac{\partial uv}{\partial y} = -\frac{\partial p}{\partial x}+\frac{1}{Re}\left(\frac{\partial^2 u}{\partial x^2}+\frac{\partial^2 u}{\partial y^2}\right), \tag{2}$$

$$\frac{\partial v}{\partial t}+\frac{\partial uv}{\partial x}+\frac{\partial v^2}{\partial y} = -\frac{\partial p}{\partial y}+\frac{1}{Re}\left(\frac{\partial^2 v}{\partial x^2}+\frac{\partial^2 v}{\partial y^2}\right), \tag{3}$$

where the dimensionless variables are defined as

$$u = \frac{\overline{u}}{U}, \quad v = \frac{\overline{v}}{U}, \quad x = \frac{\overline{x}}{A}, \quad y = \frac{\overline{y}}{A}, \quad t = \frac{\overline{t}U}{A}, \quad p = \frac{\overline{p}}{\rho U^2}, \quad Re = \frac{UA}{\nu}. \tag{4}$$

The variables with bar denote dimensional variables. Here u and v denote the Cartesian components of velocity, ν is the kinematic viscosity, ρ is the fluid density, and $L = H/A$ is the nondimensional wall to cylinder gap height.

At the far upstream, the transverse velocity component is set to zero, and a sheared profile for the longitudinal velocity component is assumed. At the plane wall and cylinder surface, no-slip boundary conditions are applied:

$$u = v = 0 \quad \text{on the cylinder,} \tag{5}$$

$$u = v = 0 \quad \text{on the plane wall } y = 0. \tag{6}$$

Further,

$$u \to y, \quad v \to 0 \quad \text{in the upstream,} \tag{7}$$

$$\frac{\partial u}{\partial x} = 0, \quad v = 0 \quad \text{at the outflow boundary.} \tag{8}$$

A zero shear boundary condition is specified along the upper boundary of the computational domain. Thus,

$$\frac{\partial u}{\partial y} = 0, \quad v = 0 \quad \text{at the top lateral boundary.} \tag{9}$$

Flow is assumed to start from rest impulsively.

A staggered grid arrangement is used to compute the flow field. In the staggered grid arrangement, the velocity components are stored at the midpoints of the cell sides to which they are normal, and the pressure is stored at the center of the cell. The continuity and momentum equations are discretized through the finite volume method over the control volumes. A typical control volume employed for the momentum and continuity equations in the staggered grid arrangement is shown in Fig. 3a–c. The convective terms at any interface of the control volume are estimated by a linear extrapolation between the two grid-point neighbors on either side of

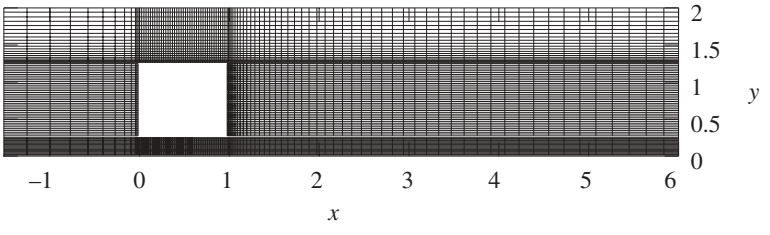

Fig. 2. The arrangement of the computational grid in the computational domain near the cylinder and plane wall for wall to cylinder gap height $L = 0.25$

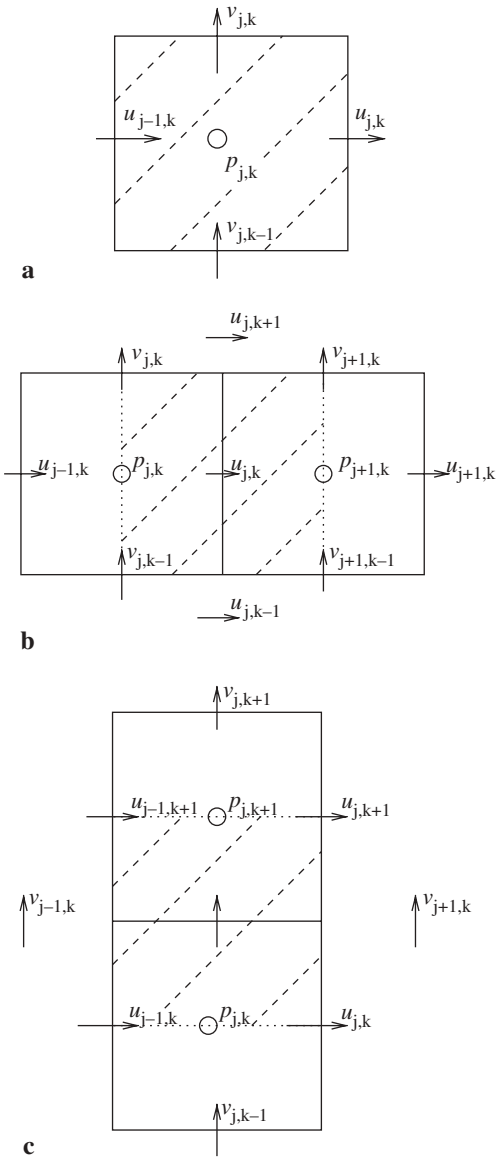

Fig. 3. Schematic of **a** p-control volume, **b** u-control volumeand, **c** v-control volume

the interface. The diffusion terms are discretized using a second-order, central difference scheme. At higher Reynolds number we have used the third-order accurate upwind differences, QUICK scheme, in the convective terms. Thus, the discretization of the space derivatives is second-order accurate.

The flow is assumed to start impulsively from rest. A forward time marching technique has been employed to compute the flow field. An implicit first order scheme is used to discretize the time derivatives present. A higher-order accurate time derivative discretization such as the three-time level implicit scheme does not produce any significant advantage. The Euler implicit scheme is computationally economical for smaller values of time steps as the three-time level implicit scheme requires storage of two previous time step solutions and the computation time is much higher. A comparison between the Euler implicit scheme and the three-time level implicit scheme has been made in our previous study [14].

A pressure correction based iteration algorithm SIMPLER (Fletcher [13]) is used for computing the discretized equations. At each time step the iteration procedure starts by supplying the previous time step solutions for velocity and pressure fields. The pressure link between the continuity and momentum is accomplished by transforming the continuity equation into a Poisson equation for pressure. The Poisson equation implements a pressure correction for a divergent velocity field. A converged solution at each time level is achieved by successively predicting and correcting the velocity components and pressure.

3 Grid considerations, and algorithm testing

A nonuniform grid distribution in the computational domain is incorporated (see Fig. 2). The grid is finer near the surfaces of the square cylinder and plane wall to better resolve the gradients near the solid surfaces. To check the grid independency we performed computations for four set of grids, namely, 185×170, 185×340, 370×170 and 370×340 with the first and second number being the number of mesh points in the x-direction and in the y-direction, respectively. The maximum distance of the first grid point from each wall is $0.01A$ and $0.005A$ for the coarse and fine grids, respectively. The effect of grid size on Strouhal number (St) and the time-average drag coefficient ($\overline{C}_D$) experienced by the cylinder at various values of the Reynolds number for uniform flow past a square cylinder placed in an unbounded region has been discussed in our earlier paper (Figs. 3a and b of [14]). We found that the changes in solution due to halving the grid size occur on the third decimal place.

At the initial stage of motion the time step δt is taken to be 0.001 which has been subsequently increased to 0.005 after the transient state. Further changes in the size of time step δt below 0.01 do not produce any significant changes in the solution. The effect of time step δt on the time average drag coefficient ($\overline{C_D}$) for different Reynolds numbers (Re) for uniform flow past a square cylinder exposed in a unbounded domain is shown in Fig. 4.

In our computation, $\delta t < \delta x$ and the velocity is always less than one except in the region between the cylinder and the ground. Clearly the Courant number ($C = |u|\frac{\delta t}{\delta x}$) is less than one in the computational domain. It assumes a maximum value 0.9 in the cells situated symmetrically between the cylinder and the wall.

The height of the top lateral boundary and outflow boundary is chosen large enough that the influence of the boundary condition on the wall shear stress is very weak. Tests were made in order to determine the suitable distances of the top boundary and downstream boundary. The outflow boundary distance is increased with an increase of Re. For a typical computation at $Re = 250$ and $L = 0.25$, for example, the top lateral boundary and outflow boundary are taken as $8A$ from the plane wall and $40A$ from the cylinder rear face, respectively.

In order to assess the accuracy of our numerical method, we have computed St and $\overline{C_D}$ for uniform flow past a square cylinder without plane wall at different values of Re and compared with the results due to Davis and Moore [15], Franke et al. [16], Treidler [17], Arnal et al. [18], Li and Humphrey [19], and Hwang and Yao [20]. A detailed discussion of errors has been made in Bhattacharyya and Maiti [14] (ref. Fig. 3).

A comparison of our computed results (St and $\overline{C}_D$) when the cylinder of height A is placed in a boundary-layer thickness δ at a gap height H from a wall has been compared with Hwang and Yao [20]. The boundary-layer flow is generated from a uniform stream over a flat plate. Table 1 displays the comparison for various values of $\frac{\delta}{A}$ and $L = \frac{H}{A}$ at $Re = 1000$. Our results are in excellent agreement with the results of Hwang and Yao [20].

Table 1. Comparison of Strouhal number (St) and time-average drag coefficient ($\overline{C}_D$) at $Re = 1000$ and for boundary-layer thickness $\frac{\delta}{A} = 0.8, 5.0$ at various gap heights L

Configuration		Strouhal number (St)			Drag coefficient ($\overline{C}_D$)		
$\frac{\delta}{A}$	L	Present	Hwang et al. [20]	%Error	Present	Hwang et al. [20]	%Error
0.8	5.5	0.121	0.122	1.64	1.99	1.98	0.50
	3.5	0.121	0.124	2.41	1.97	1.97	0.00
	1.5	0.132	0.135	2.22	2.13	2.14	0.46
	1.0	0.144	0.140	2.86	2.10	2.15	2.36
5.0	5.5	0.122	0.121	0.82	1.97	1.94	1.54
	3.5	0.106	0.111	4.50	1.64	1.66	1.21
	1.5	0.086	0.088	2.27	0.80	0.79	1.26
	1.0	0.083	0.080	3.75	0.52	0.50	4.00

4 Results and discussions

The present flow field is governed by two parameters, namely, the Reynolds number Re and wall to cylinder gap heights L. We have presented the numerical solutions for wall to cylinder gap heights $L = 0.25$, 0.2, 0.15 and 0.1 at different values of the Reynolds number.

The time evolution of the velocity components (u, v) at the point which is on the centerline of the cylinder and just off the rear face of the cylinder (the location of the monitor point is indicated in Fig. 1) for wall to cylinder gap heights $L = 0.25$, 0.2, 0.15, 0.1 at $Re = 250$ shows that the flow field reaches a steady state at this Reynolds number after an initial transition. The time history of the velocity field is not shown here for the sake of brevity. The vorticity contours for the steady flow at the wall to cylinder gap height $L = 0.25$ are shown in Fig. 5 when $Re = 250$. It shows that in the vicinity of the cylinder and the plane wall there are three shear layers; the two shear layers that develop near the surface of the cylinder on the top and bottom, respectively, and the shear layer that develops along the plane wall. The upper shear layer on

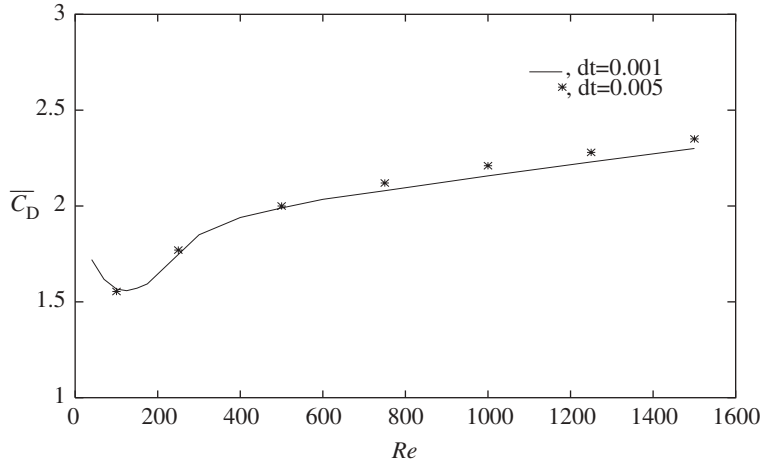

Fig. 4. The effect of time step δt on time average drag coefficient ($\overline{C_D}$) for different Reynolds numbers (Re) for uniform flow past a square cylinder placed in an unbounded domain

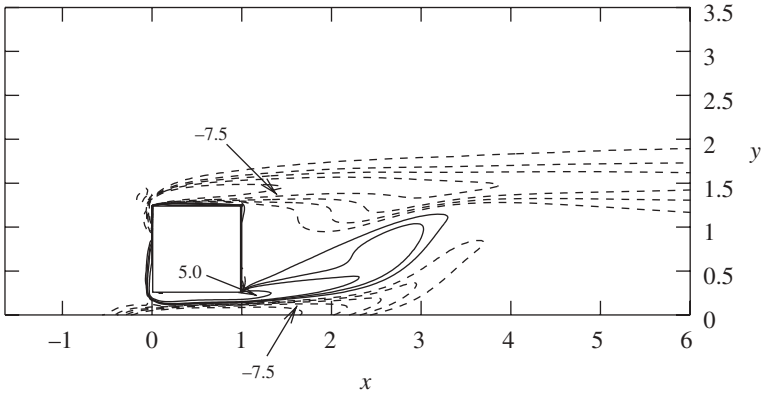

Fig. 5. Vorticity contours for wall to cylinder gap height $L = 0.25$ at $Re = 250$. The negative vortex lines are denoted by dashed lines and positive vortex lines are denoted by solid lines

the cylinder and the shear layer on the plane wall has negative vorticity and is indicated by dashed lines, whereas the lower shear layer on the cylinder has positive vorticity and is indicated by solid lines. It is clear from the figure that the vortex shedding is suppressed at this Reynolds number and the wake behind the cylinder is steady. The thick wall boundary layer at low Reynolds number interacts with the cylinder lower shear layer and diffuses part of the positive vorticity in the lower shear layer. Consequently this lower shear layer is not strong enough to influence the negative upper shear layer. The upper shear layer thus convects downstream without being roll-up, and the weak lower shear layer reattaches with the cylinder lower face without shedding.

The form of the wake at the lower value of wall to cylinder gap height $L = 0.1$ is described in Fig. 6 for $Re = 350$. We find that the wake is steady at this value of Reynolds number with $L = 0.1$. The upper shear layer emerges from the top of the cylinder transported downstream almost horizontally without forming any vortex in the near wake of the cylinder. The negative wall boundary layer interacts with the positive shear layer induced by the cylinder wall face and greatly reduces its strength. The wall boundary layer separates in the downstream of the cylinder and the separation point shifts further downstream at an increased value of the Reynolds number.

Figure 7 shows the pressure distribution (C_p) along the cylinder surface at $Re = 250$ for gap height $L = 0.25, 0.2, 0.15, 0.1$. The pressure is positive along the windward face of the cylinder. A separated pressure distribution occurs along the bottom face and side face of the cylinder. It may be noted that at gap height higher than 0.3 the negative pressure (base suction) occurs near the front corner of the bottom face of the cylinder, and the flow encounters an adverse pressure gradient in the gap region [2]. On the contrary, our result for $L \leq 0.25$ at $Re = 250$ shows that fluid moves with the pressure gradient in the gap region.

The underbody flow at $Re = 200, 400$ for wall to cylinder gap heights $L = 0.25, 0.1$ is presented in Figs. 8 and 9. The time histories of velocity components (not presented for the sake of brevity) show that the wake is steady for these cases. Figure 9 depicts the pressure distribution along the wall side face of the cylinder and along the plane wall in the gap region. Figure 9a and b shows that the pressure distribution (C_p) difference between the sides is almost zero in the core of the gap region for $L = 0.1, 0.25$ at $Re = 200, 400$. This implies that for smaller values of wall to cylinder gap height the gap flow is unidirectional, and the core flow resembles that of channel flow. This result agrees with the experimental

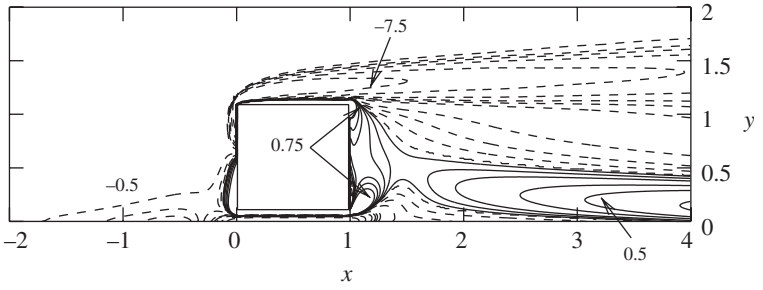

Fig. 6. Vorticity contours for wall to cylinder gap height $L = 0.1$ at $Re = 350$. The negative vortex lines are denoted by dashed lines and positive vortex lines are denoted by solid lines

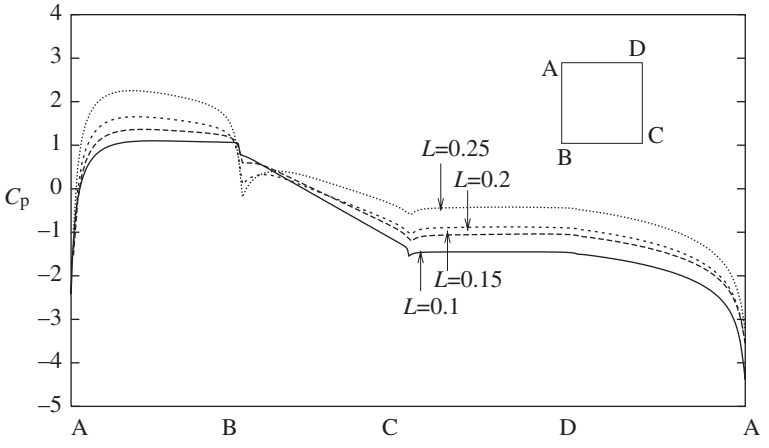

Fig. 7. Pressure distribution (C_p) over the cylinder for wall to cylinder gap heights $L = 0.25$, $0.2, 0.15, 0.1$ at $Re = 250$

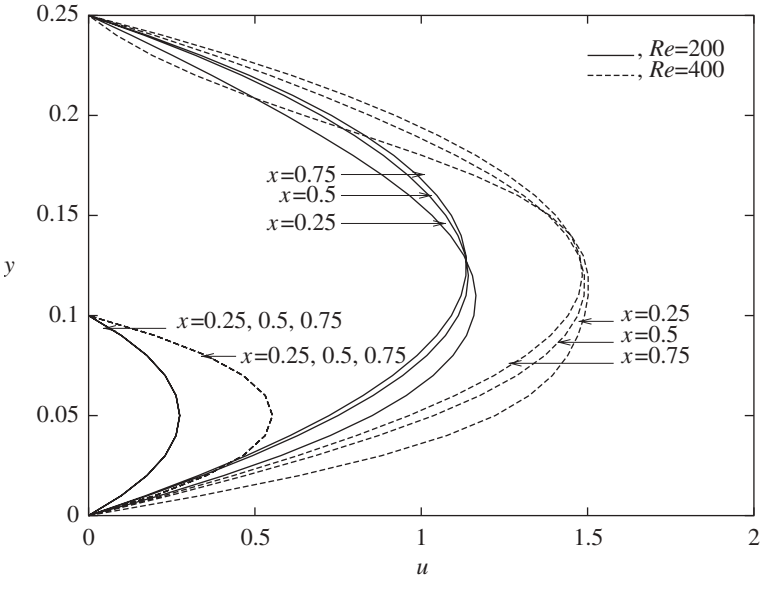

Fig. 8. u-velocity profiles in the gap flow for wall to cylinder gap heights $L = 0.25, 0.1$ at $Re = 200, 400$

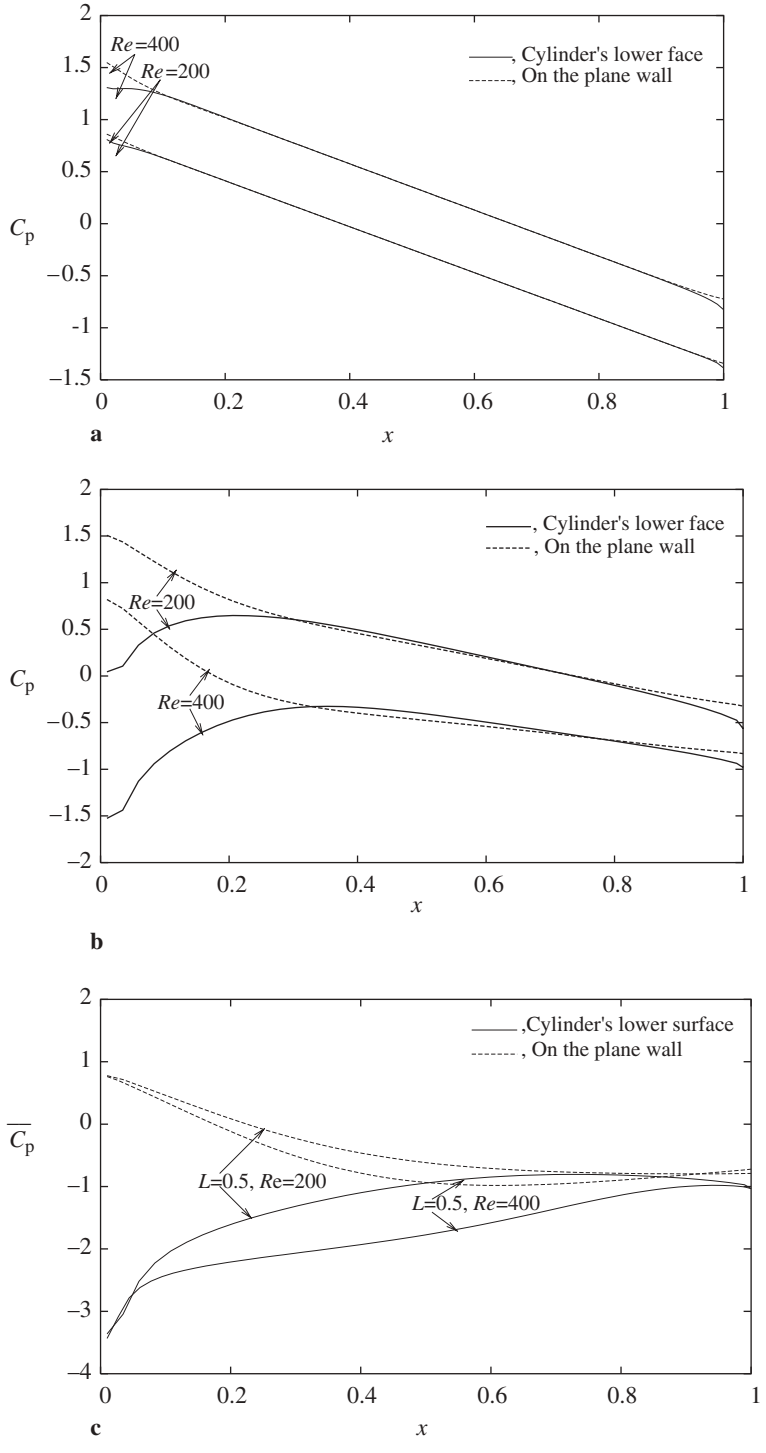

Fig. 9. **a** Pressure distribution (C_p) on cylinder's lower face and on the plane wall for gap heights $L = 0.1$ at $Re = 200, 400$; **b** pressure distribution (C_p) on cylinder's lower face and on the plane wall for gap heights $L = 0.25$ at $Re = 200, 400$; **c** Time average pressure distribution ($\overline{C_p}$) on cylinder's lower face and on the plane wall for gap height $L = 0.5$ at $Re = 200, 400$

finding of Martinuzzi et al. [10]. We have presented the time average pressure distribution $(\overline{C_p})$ along the wall side face of the cylinder and along the plane wall in the gap region for gap height $L = 0.5$ at $Re = 200, 400$ in Fig. 9c. It may be noted that for this gap height $L = 0.5$ at $Re = 200, 400$ the wake is periodic and consist of an upper row of strong negative vortices and lower row of weak positive vortices. Our result shows that when $L > 0.25$, the bottom face pressure is less than the pressure along the wall. Our result agrees qualitatively with the Martinuzzi et al. [10] pressure measurement. There they have argued through inviscid analysis that when the pressure distribution along the bottom face is less than the pressure distribution along the wall, the streamline curvature below the bottom face is positive with respect to the lower face. When the streamline curvature is positive, the upper and lower shear layers of the cylinder are strongly coupled. The interaction of these shear layers result in a regular vortex shedding behind the body.

The horizontal component of velocity profile at different x-station $(x = 0.25, 0.5, 0.75)$ within the gap region is presented in Fig. 8. The perpendicular velocity (v) is almost negligible, and the horizontal velocity (u) takes a parabolic form. The magnitude of the velocity in the gap flow increases with the increase of the Reynolds number. It may be noted that at higher values of wall to cylinder gap height L the velocity profiles overshoot, and a strong gap flow generates [21].

Effects of higher Reynolds number ($Re \geq 500$) on the flow at different values of wall to cylinder gap height are shown in Figs. 10–13. At $Re = 500$, the time histories of the velocity components (u, v) at the monitor point (the location of the point is indicated in Fig. 1) is presented in Figs. 10a and b for wall to cylinder gap heights $L = 0.25, 0.2, 0.15$ and 0.1. It shows that the wake is periodic at $Re = 500$ for $L = 0.25$. A weak periodicity occurs for wall to cylinder gap height $L = 0.2$. But the wake is steady at $L = 0.15$ and 0.1 for $Re = 500$. This may be due to the fact that at higher Re the wall boundary-layer thickness reduces and for wall to cylinder gap heights $L \geq 0.2$ the interaction with the cylinder upper shear layer is not strong enough to prevent rolling-up. Figures 10c and d show that the flow field is periodic at $Re = 700$ when the gap height is $L = 0.2$.

Figure 11 shows the vorticity contours at wall to cylinder gap height $L = 0.25$ for high values of Reynolds number $Re = 500$. The result shows that at this high value of Reynolds number the upper shear layer rolls-up in a periodic manner and the wake consists of a single row of negative vortices. The wall boundary layer diffuses the positive vortex induced by the cylinder lower shear layer and reduces the circulation, which delays the roll-up into a well-defined positive vortex. The periodicity in the wake associated with the shear layer originates from the upper side of the cylinder. Earlier Price et al. [6] also observed the same phenomena for the case of a circular cylinder placed close to a wall.

The vorticity contours at wall to cylinder gap height $L = 0.2$ and 0.25 for Reynolds number $Re = 700$ are shown in Figs. 12 and 13. The flow field is periodic at these values of the parameter. The wake consists of a single row of negative vortices. The flow separation and formation of large eddies on the plane wall in the downstream of the cylinder occurs at this lower gap height $L = 0.2$ for higher values of the Reynolds number $Re = 700$.

5 Conclusions

The uniform shear flow past a square cylinder placed close to a plane wall has been investigated numerically for Reynolds numbers (Re) up to 700 and at different values of wall to cylinder gap

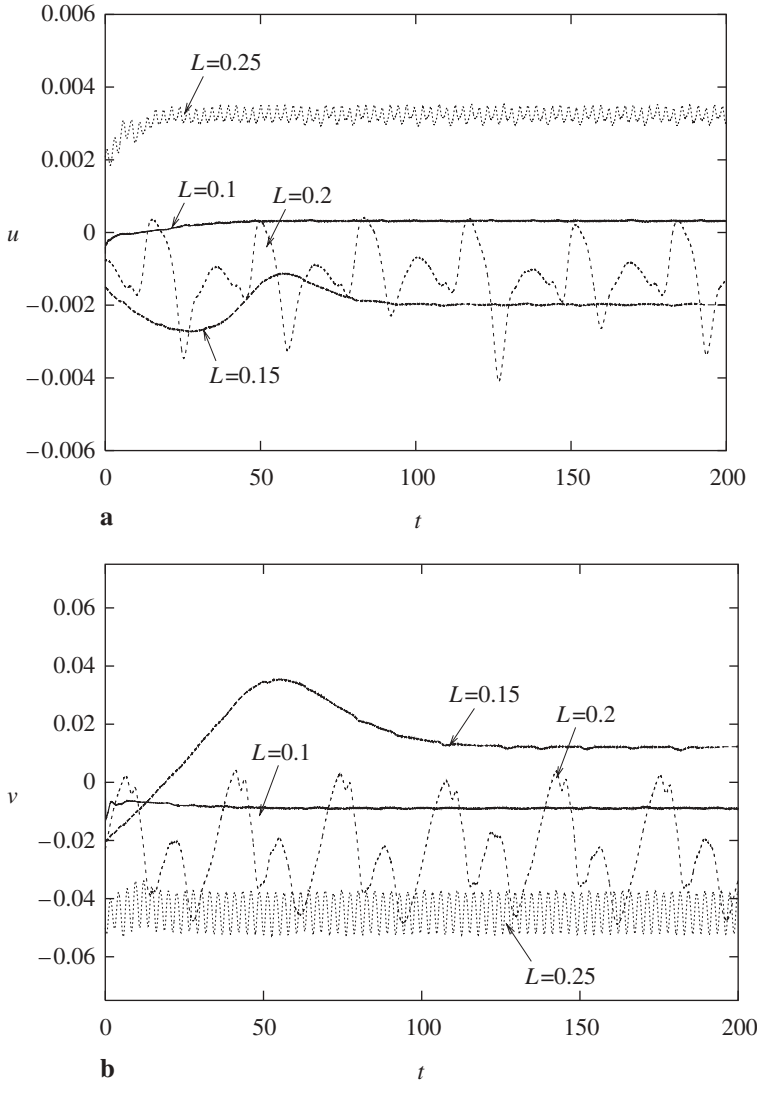

Fig. 10. Time history of velocity components (u, v) at the location of monitor point for wall to cylinder gap heights $L = 0.25, 0.2, 0.15$ and 0.1 at $Re = 500$ and 700: **a** u-velocity component, $Re = 500$; **b** v-velocity component, $Re = 500$; **c** u-velocity component, $Re = 700$; **d** v-velocity component, $Re = 700$

height ($L = 0.25, 0.2, 0.15, 0.1$). The major results of the present study can be summarized as follows:

(i) At smaller values of wall to cylinder gap height ($L < 0.25$) or lower Reynolds number ($Re < 500$) vortex shedding is suppressed, and the wake behind the cylinder is steady. The thick wall shear layer of negative vortices interacts with the positive vorticity induced by the cylinder lower shear layer. The cylinder lower shear layer reattaches to the cylinder itself, and the upper shear layer convects downstream almost horizontally without being roll-up.

(ii) The gap flow near the trailing edge of the cylinder when vortex shedding is suppressed is almost unidirectional and similar to a channel flow.

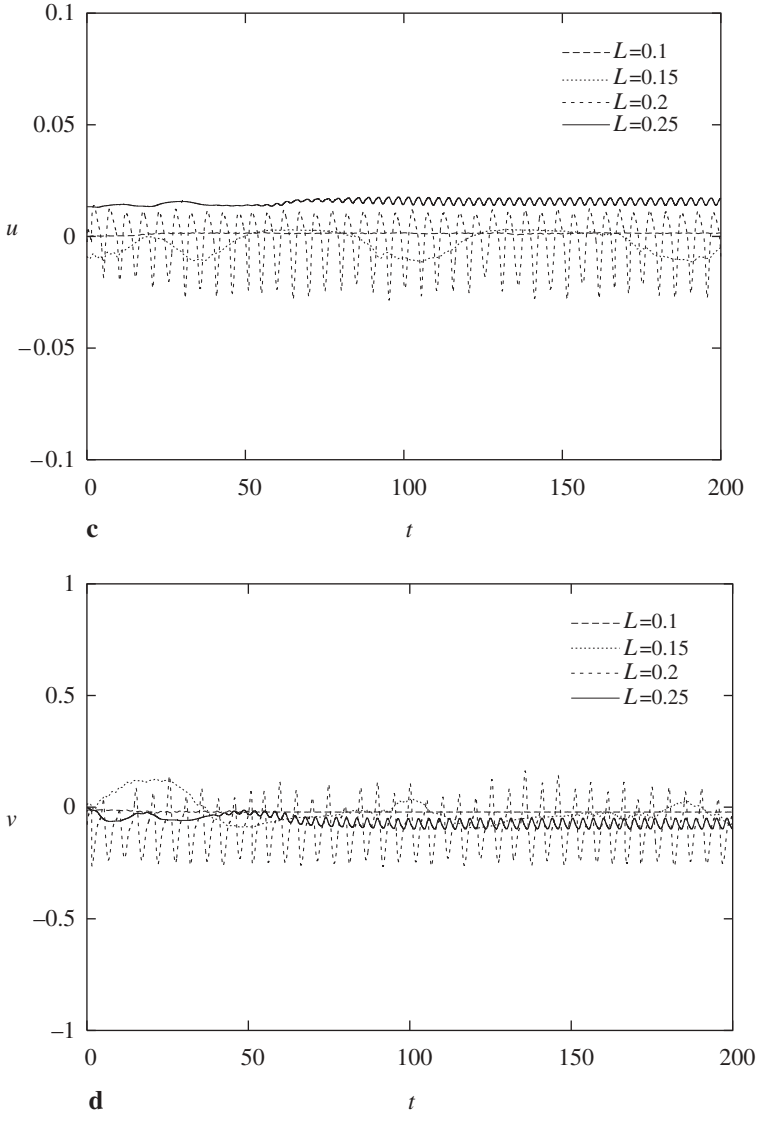

Fig. 10. (Contd.)

(iii) At the lower values of wall to cylinder gap heights, the separation bubble appears in the upstream of the cylinder.
(iv) At large Reynolds number ($Re \geq 500$) the wake consist of a single row of counter rotating vortices induced by the cylinder upper shear layer.
(v) The critical value of wall to cylinder gap height for vortex shedding suppression decreased as the on-coming boundary layer increased.

It may be noted that several authors (e.g., Bosch and Rodi [4], and Bosch et al. [9], Bailey et al. [1], Martinuzzi et al. [10]) considered the turbulent flow behind a square cylinder near a wall and observed that the vortex shedding suppression is much less sensitive to the oncoming

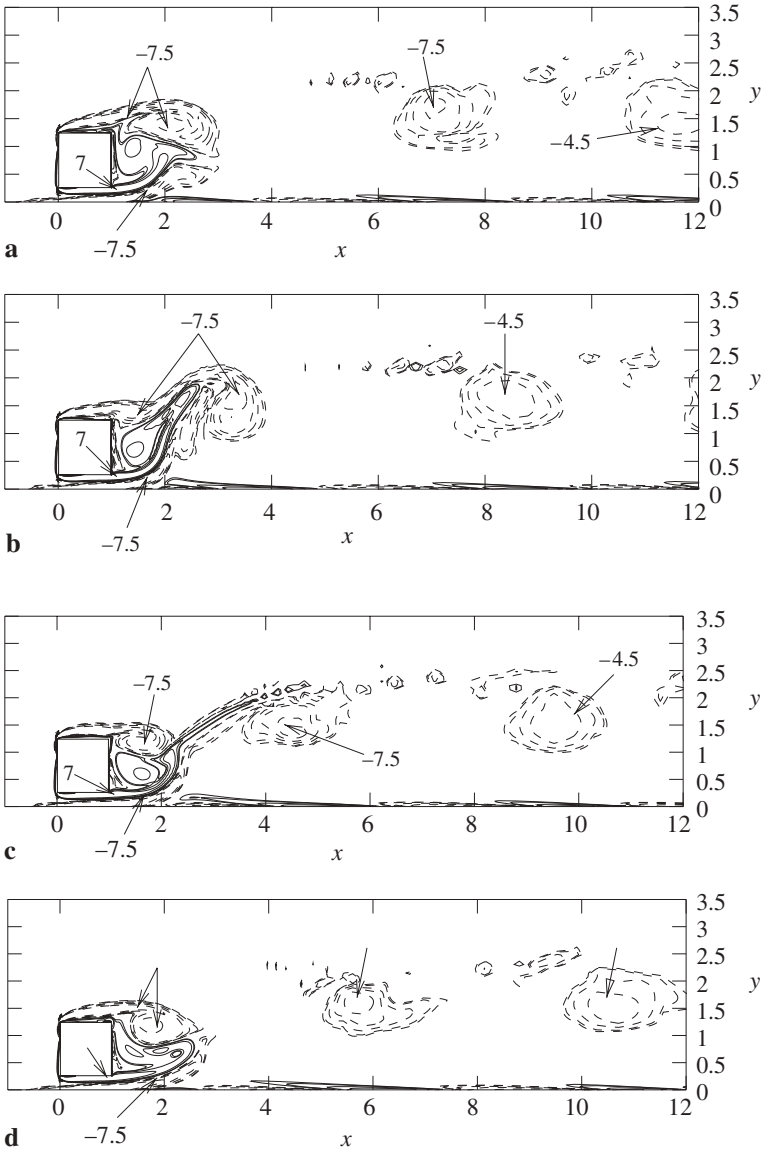

Fig. 11. Vorticity contours for wall to cylinder gap height $L = 0.25$ and $Re = 500$. The negative vortex lines are denoted by dashed lines and positive vortex lines are denoted by solid lines; **a** $t = T$; **b** $t = T + T/4$; **c** $t = T + T/2$; **d** $t = T + 3T/4$

boundary layer thickness. We found that the vortex shedding suppression depends on the wall boundary layer thickness as well as cylinder to wall gap height. Our result shows that the reattachment process of the separated shear layer on the wall side face interrupts the vortex feedback mechanism and vortex shedding is suppressed.

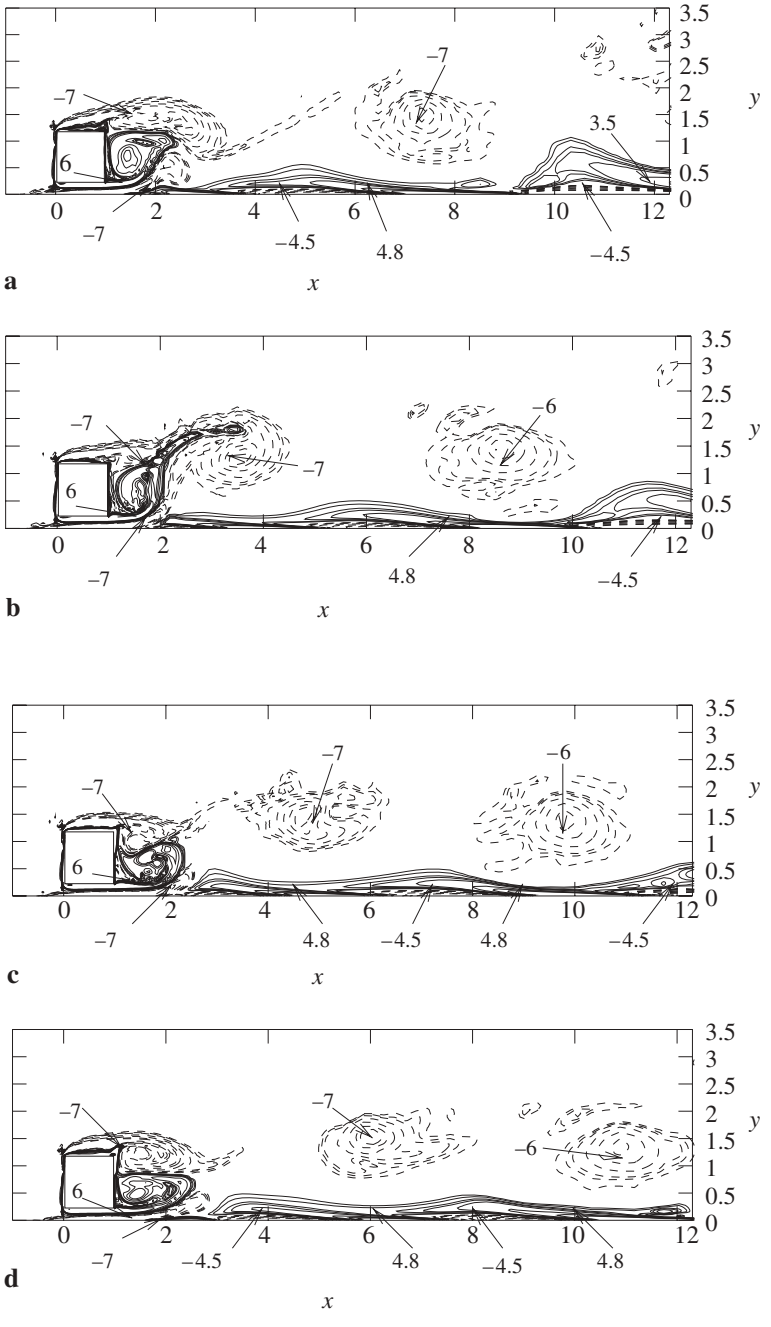

Fig. 12. Vorticity contours for wall to cylinder gap height $L = 0.2$ and $Re = 700$. The negative vortex lines are denoted by dashed lines and positive vortex lines are denoted by solid lines: **a** $t = T$; **b** $t = T + T/4$; **c** $t = T + T/2$; **d** $t = T + 3T/4$

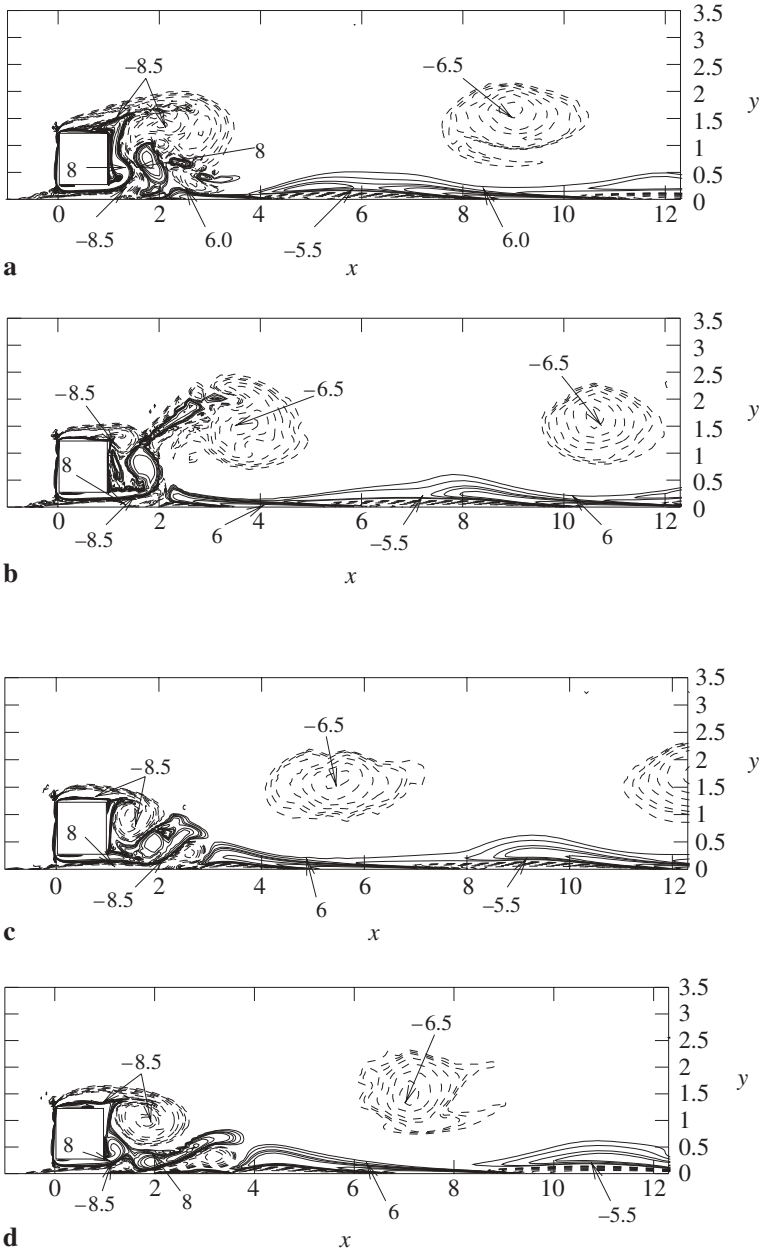

Fig. 13. Vorticity contours for wall to cylinder gap height $L = 0.25$ and $Re = 700$. The negative vortex lines are denoted by dashed lines and positive vortex lines are denoted by solid lines. **a** $t = T$; **b** $t = T + T/4$; **c** $t = T + T/2$; **d** $t = T + 3T/4$

Acknowledgements

One of the authors (S. B.) wishes to thank the Department of Science and Technology, Government of India for providing financial support through a research project grant.

References

[1] Bailey, S. C. C., Martinuzzi, R. J., Kopp, G. A.: The effect of wall proximity on vortex shedding from a square cylinder: Three-dimensional effects. Phys. Fluids **14**, 4160–4176 (2002).
[2] Bearman, P. W., Zdravkovich, M. M.: Flow around a circular cylinder near a plane boundary. J. Fluid Mech. **89**, 33–47 (1978).
[3] Taniguchi, S., Miyakoshi, K., Dodhda, S.: Interference between plane wall and two-dimensional rectangular cylinder. Trans. JSME **49-447**, 2522–2529 (1983).
[4] Bosch, G., Rodi, W.: Simulation of vortex shedding past a square cylinder near a wall. Int. J. Heat Fluid Flow **17**, 267–275 (1996).
[5] Zovatto, L., Pedrizzetti, G.: Flow about a circular cylinder between parallel walls. J. Fluid Mech. **440**, 1–25 (2001).
[6] Price, S. J., Sumner, D., Smith, J. G., Leong, L., Paidoussis, M. P.: Flow visualization around a circular cylinder near to a plane wall. J. Fluids Struct. **16**, 175–191 (2002).
[7] Grass, A. J., Raven, P. W. J., Stuart, R. J., Bray, J. A.: The influence of boundary layer velocity gradients and bed proximity on vortex shedding from free spanning pipelines. J. Energy Resources Tech. ASME Trans. **106**, 70–78 (1984).
[8] Taneda, S.: Experimental investigations of vortex streets. J. Phys. Soc. Japan. **20**, 1714–1721 (1965).
[9] Bosch, G., Kappler, M., Rodi, W.: Experiments on the flow past a square cylinder placed near a wall. Exp. Therm. Fluid Sci. **13**, 292–305 (1996).
[10] Martinuzzi, R. J., Bailey, S. C. C. R., Kopp, G. A.: Influence of wall proximity on vortex shedding from a square cylinder. Experiments Fluids **34**, 585–596 (2003).
[11] Liou, T., Chen, S., Hwang, P.: Large eddy simulation of turbulent wake behind a square cylinder with a nearby wall. J. Fluid Engng. **124**, 81–90 (2002).
[12] Lei, C., Cheng, L., Armfield, S. W., Kavanagh, K.: Vortex shedding suppression for flow over a circular cylinder near a plane boundary. Ocean Engng. **27**, 1109–1127 (2000).
[13] Fletcher, C. A. J.: Computational techniques for fluid dynamics -I, II. Springer Ser. Comput. Phys. Berlin Heidelberg: Spinger 1991.
[14] Bhattacharyya, S., Maiti, D. K.: Vortex shedding from a square cylinder in presence of a moving ground. Int. J. Numer. Meth. Fluids **48**, 985–1000 (2005).
[15] Davis, R. W., Moore, E. F.: A numerical study of vortex shedding from rectangles. J. Fluid Mech. **116**, 475–506 (1982).
[16] Franke, R., Rodi, W.: Numerical calculation of laminar vortex shedding flow past cylinders. J. Wind Engng. Ind. Aero. **35**, 237–257 (1990).
[17] Treidler, E. B.: An experimental and numerical investigation of flow past ribs in channel. Ph.D Thesis, University of California at Berkeley, CA, 1991.
[18] Arnal, M. P., Georing, D. J., Humphrey, J. A. C.: Vortex shedding from a bluff body on a sliding wall. J. Fluid Engng. **113**, 384–398 (1991).
[19] Li, G., Humphrey, J. A. C.: Numerical modelling of confined flow past a cylinder of square cross-section at various orientations. Int. J. Numer. Meth. Fluids **20**, 1215–1236 (1995).
[20] Hwang, R. R., Yao, C.: A numerical study of vortex shedding from a square cylinder with ground effect. J. Fluid Engng. **119**, 512–518 (1997).
[21] Jones, M. A., Smith, F. T.: Fluid motion for car undertrays in ground effect. J. Engng. Math. **45**, 309–334 (2003).

Authors' addresses: S. Bhattacharyya, Department of Mathematics, Indian Institute of Technology, Kharagpur 721302, India; D. K. Maiti, Department of Mathematics, Birla Institute of Technology and Science, Pilani 333031, India (E-mail: somnath@maths.iitkgp.ernet.in)